

The nonlinear inversion of paleogeothermal evolution: An example from the northern part of the South China Sea

XUE AIMIN

Institute of Geophysics, Chinese Academy of Sciences
Tatun Road, Beijing 100101, P.R. China

Abstract: The paleogeothermal history inversion method is studied in this paper. The thermal model implies variation of basal heat flow with time, and thermal conductivity with sediment porosity and composition. The thermal evolution as a nonlinear function can be represented by segments of linear functions in which each segment reflects a tectonic stage. The technique of inversion including the Simplex and Monte Carlo methods have been used for the calculation of geothermal evolution and the comparison of the calculated and observed vitrinite reflectances.

The application of nonlinear inversion method has been illustrated in the research of geothermal history for the northern part of South China Sea. The results including tectonic and geothermal histories suggest that most of the oil-bearing rocks in the area are mature and overmature and at least two or three extensions have occurred since the Later Mesozoic period.

INTRODUCTION

Hydrocarbon generation depends upon time and temperature (Waples, 1980). One of the important research tasks in sedimentary basin analysis is to give the geothermal history. During the past 30 years, many geologists have attempted to establish numerical models of geothermal evolution of basins with some different approaches (Lopatin, 1971; Waple, 1980; Nunn *et al.*, 1984; McKenzie, 1978; Royden *et al.*, 1980; Lerche *et al.*, 1984, Lerche 1988a, Lerche 1988b; Pantano and Lerche, 1990). Some of the models were built from the research of dynamics and mechanics of basin subsidence, and others from the research of geochemistry, organic maturation and some geological thermal indicators. The former models involve the detailed structure and the mechanics of basin subsidence, but the latter models do not address the burial subsidence mechanics of the basins.

The complication of using the models is that they rely on accurate knowledge of the burial history and geological and geothermal parameters to determine paleotemperatures. It is possible to reconstruct burial history and geological and geothermal parameters of basins. Parameters of the burial history can be determined more reliably than that of the subsidence mechanics. The inversion of geothermal history in this paper depends on the nonlinear inversion approach of mathematics, vitrinite reflectance R_0 which indicates the organic maturation, tectonic structures which are related to the evolutionary stages, and geological and geothermal parameters.

The approach of inversion of paleogeothermal temperature has been developed through the works of Waples (1980), Lerche *et al.* (1984), and Lerche (1988a, 1988b). In this paper, the author follows inversion technique of Lutz and Omar (1991) using apatite fission track data. It is a combination of Simplex and Monte Carlo methods. The example of inversion of geothermal evolution in the north part of South China Sea is presented.

THE METHOD OF INVERSION

Lerche (1984) has advanced a new method to inverse paleo-heat flux. The function which describe the relationship between heat flux and time is as followed:

$$Q(t) = Q_0 (1 + \beta t) \quad \dots\dots\dots(1)$$

where

Q_0 = recent heat flux,

t = geological time measured from present,

β = constant

The function gives a linear variation of heat flux with time, which represents a single tectonic heating event. If we regard the nonlinear heat flux related to tectonic evolution as a series of linear functions, we have:

$$Q_1(t) = Q_0 (1 + \beta_1 \cdot t), \quad \text{as } t_1 > t \geq t_0, t_0 = 0$$

$$Q_2(t) = Q(t_1) \cdot [1 + \beta_2 \cdot (t - t_1)], \quad \text{as } t_2 > t \geq t_1$$

·

·

·

$$Q_n(t) = Q_{n-1}(t_{n-1}) \cdot [1 + \beta_n \cdot (t - t_{n-1})], \text{ as } t_n > t \geq t_{n-1}, \dots (2)$$

The paleotemperature can be described as:

$$T_1(t) = T_{1s} + Q_1(t) \cdot \int_0^{z(t)} \frac{dZ'}{K_{pr}(Z')}, \quad \text{as } t_1 > t \geq 0$$

$$T_2(t) = T_{2s} + Q_2(t) \cdot \int_0^{z(t)} \frac{dZ'}{K_{pr}(Z')}, \quad \text{as } t_2 > t \geq t_1$$

$$T_n(t) = T_{ns} + Q_n(t) \cdot \int_0^{z(t)} \frac{dZ'}{K_{pr}(Z')}, \quad \text{as } t_n > t \geq t_{n-1} \dots (3)$$

where $Q_0, Q_1(t_1), \dots, Q_{n-1}(t_{n-1})$ are the heat flux at the start point of tectonic stages, t_0, t_1, \dots, t_{n-1} ; $T_{1s}, T_{2s}, \dots, T_{ns}$ are the surface temperatures in the tectonic stages, which can be regarded as 0°C for simplicity of the computation; $Z(t)$ is the profile of subsidence history in the basin and $K_{pz}(z)$ is the thermal conductivity mentioned above. What we want to compute is the evolutionary profile of geothermal temperatures. If we extrapolate the paleothermal temperature between the tectonic stages, we produce the geothermal evolutionary profile. The extrapolated segments can be expressed to be the thermal indicators. In the paper, the vitrinite reflectance R_0 has been used.

The models of the relationship of R_0 to time-temperature-indicator (TTI) and the relationship of TTI to time and temperature are taken from the previous research work (Wood, 1988). The object function of inversion can be described as:

$$X(Q_1, Q_2, \dots, Q_n) = \sum_{k=1}^m [R_{0k} - R'_{0k}]^2 / m]^{1/2} \dots (4)$$

If X is as small as we expected, the geothermal history profile is selected. But it is not easy to get a reliable geothermal history profile as the result of the inversion are multivalued functions of time. The different initial values of inversion could give different results, but the best results would relate to the smallest object function value. Based on the analysis above, the author employed the Monte Carlo method to produce the initial values of thermal history inversion that ranged from the smallest value to the largest value estimated from geological information. The Monte Carlo initial value box is shown in Figure 1.

After deriving the initial values of heat flux, the Simplex Method can be employed to inverse the appropriate geothermal temperatures. The Simplex Method is a simple but effective method in inversion theory and detailed descriptions are found in many mathematical books (Press *et al.*, 1986). Lutz and Omar (1991) have used the Monte Carlo and

Simplex Method to calculate thermal history using apatite fission track data. The author will not describe in detail as the difference of inversion method is only in the thermal temperature recorders that we selected.

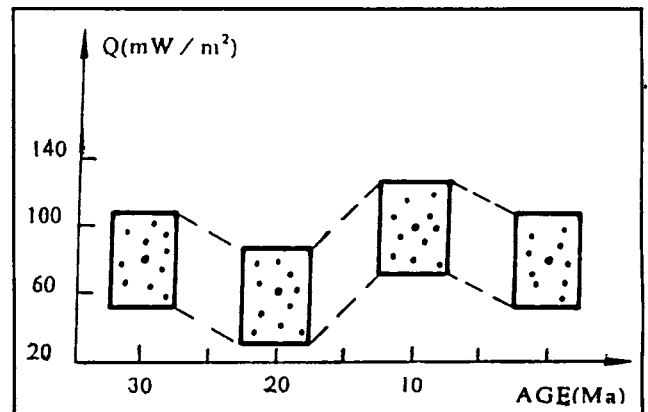


Figure 1. The Monte Carlo box of heating flux and age.

GEOLOGY AND THERMAL HISTORY MODELS OF NORTHERN PART OF SOUTH CHINA SEA

The thermal history of the northern part of South China Sea has been studied. The geological setting of northern part of South China Sea is shown in Figure 2. The sedimentary basins located on the area are Pearl River Mouth Basin, Yingge Sea Basin, Qong Southeast Basin and Beibu Gulf Basin.

The beginning of the basin subsidence dates from Late Cretaceous (Ru and Pigott, 1985, 1986, 1988). A coarse-grained red sandstone, hundreds meters in thickness, covered the basal rocks which represented by the rocks various pre-Late Cretaceous rocks.

Ru and Pigott (1988) has indicated that the extension could be divided into three stages; each representing a special tectonic event. The first stage in Late Cretaceous, is the time of velocity decrease of plate convergence which began in middle Jurassic along the coast of South China continent where the northern part of South China Sea is located now (Ru and Pigott, 1988). The second stage in Late Eocene, coincides with the initiation of collision between the Indian Plate and Eurasian Plate. The third stage in middle Miocene coincides with the orogeny event that formed the Himalayas. The time of the unconformity of breaking up in Yingge Sea-Qong Southeast Basin is about early Oligocene. It must be pointed out that the thickness of thousands meters of Pleistocene sediments in Yingge Sea Basin-Qong Southeast Basin may reflect

tectonic events of this age associated with the activities between Indochina and Eurasia continents. The post-rifting sediments filled in all the basins in the area

Figures 3 and 4 show the sedimentary characteristics of Yingge Sea Basin and Beibu Gulf Basin. It must be pointed out that the great thickness of sediments and their deposition environment as well as their structures indicate that the mechanics of subsidence are different from other basins in the area. Many mud-diapirs have been found in Yingge Sea Basin. The thick black shales form structural traps to create favourable prospect for oil and gas exploration in the basins.

The heat flux of the basins, ranging from 61.7-62.2 mw/m² indicates that the basins of northern part of South China Sea have similar recent thermal history (Li and Huang, 1990a). The geothermal gradients are different in different basins, which could be interpreted as due to local variation in fluid activities and conductivities. The thermal history models of the areas are shown in Tables 1 and 2.

The method developed by Sass *et al.* (1971) had been used here in the analyses of thermal conductivities:

$$K_{pr} = K_w \cdot K_{mT}^{1-\varphi} \quad \dots\dots (5)$$

and

$$K_{mT} = K_{m20} \cdot [293/(T + 273)] \quad \dots\dots (6)$$

where

K_{pr} = the *in-situ* thermal conductivity of a porous rocks;

K_{mT} = the matrix conductivity at the *in-situ* temperature;

K_w = the conductivity of water;

K_{m20} = the matrix conductivity at 20°C;

t = temperature in °C;

φ = porosity.

Because there is very little porosity data from the region, the porosity-depth function (Allen and Allen, 1990) is used in the form of:

$$\varphi = \varphi_0 \cdot \exp(-Cz) \quad \dots\dots (7)$$

where

φ_0 = porosity estimated at zero depth (Table 1, 2)

C = constant of decreasing depth, z (Table 1, 2)

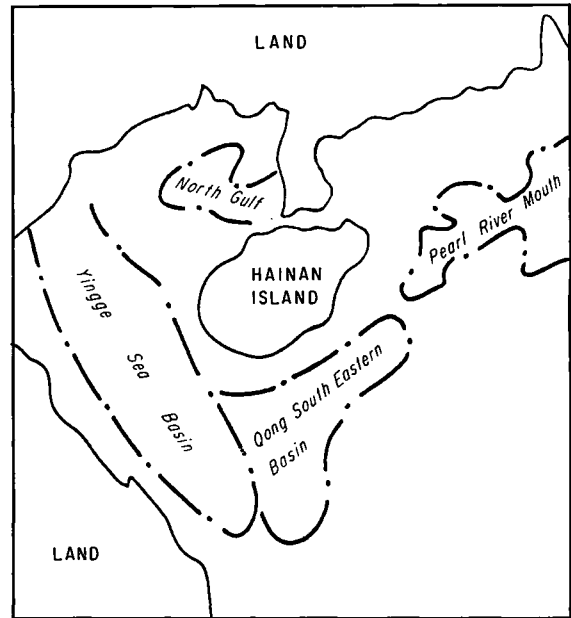


Figure 2. The geological setting of the northern part of the South China Sea Basin.

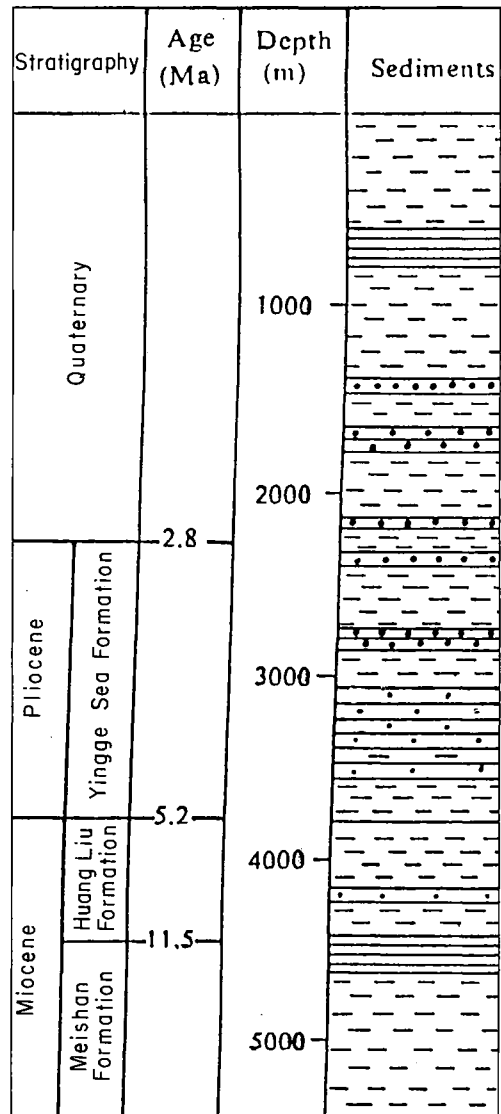


Figure 3. The stratigraphy of Yingge Sea Basin.

Table 1: Thermal history model of Yangge Sea Basin.

Stratigraphy (sediments)	Matrix Conductivity (W/m.K)		Porosity at Earth Surface ϕ_0	Porosity Decrease factor with depth, C (km ⁻¹)	Vitrinite Reflectance Ro (%)	
	Reference	Range*			Reference	Range*
Quaternary (mudstone, sandy siltstone)	2.50	2.0-3.4	0.50	0.41	0.47	0.43-0.6
Yingge Sea Formation (up) (mudstone, local sandstone)	2.65	2.0-3.4	0.47	0.4	0.92	0.6-1.3
Yingge Sea Formation (lower) (mudstone and sandstone)	2.65	2.0-3.4	0.47	0.4	1.28	0.7-1.5
Huang Liu Formation (up) (mudstone, sandstone)	2.65	2.0-3.4	0.47	0.4	1.55	0.8-1.7
Huang Liu Formation (lower) (sandy mudstone, sandstone)	2.55	2.0-3.4	0.50	0.4	1.76	1.45-1.8
Meishan Formation (mudstone, sandy mudstone, sandstone)	2.55	2.0-3.4	0.50	0.4	2.65	2.2-2.8

*Range from Fig. 1 and Fig. 4 (Li and Huang, 1990);
 ϕ_0 and C estimated from logging data of some areas;
Ro (%) include data from Quong Southeast Basin.

Table 2: Thermal history model of North Gulf Basin.

Stratigraphy (sediments)	Matrix Conductivity (W/m.K)		Porosity at Earth Surface ϕ_0	Porosity Decrease factor with depth, C (km ⁻¹)	Vitrinite Reflectance Ro (%)	
	Reference	Range*			Reference	Range*
Jiaowai Formation (sandy siltstone, sandstone)	2.55	2.0-3.4	0.47	0.4	0.32	0.31-0.42
Xianyang Formation (sandstone, conglomerate, mudstone)	2.65	2.0-3.4	0.47	0.4	0.34	0.3-0.45
Weizhou Formation, Upper member (mudstone, conglomerate, sandstone)	2.65	2.0-3.4	0.47	0.4	0.39	0.34-0.51
Weizhou Formation, Lower member (mudstone, conglomerate, sandstone)	2.65	2.0-3.4	0.47	0.4	0.52	0.31-0.55
Liushagang Formation, First member (mudstone and sandstone)	2.6	2.0-3.4	0.47	0.4	0.64	0.5-0.9
Liushagang Formation, Second member (black shale and sandy siltstone)	2.5	2.0-3.4	0.47	0.4	0.98	0.6-1.1
Liushagang Formation, Third member (shale and sandstone)	2.6	2.0-3.4	0.47	0.4	1.3	1.3

* Range: 2.0W/m.K = mudstone matrix conductivity;
3.4W/m.K = sandstone matrix conductivity;
Ro (%) is from Fig.3 (Li and Huang., 1990);
 ϕ_0 and C is estimated from logging data of some areas.

Stratigraphy		Reflective Layer	Age(Ma)	Depth(m)	Sediments
Miocene	A	T ₁	17	440	[Sediment pattern]
	B				
Mid-Upper Oligocene	C	T ₂	23.8	630	[Sediment pattern]
	Lower Oligocene	D	T ₃ (T' ₃)	28	1230
Mid-Up Eocene		E	T ₄ (T' ₄)	32	1845
	Lower Eocene Up Palaeocene	F	T ₅	37	2320
G		T ₆	41	2930	[Sediment pattern]
		T ₇	51	3660	[Sediment pattern]

Figure 4. The stratigraphy of North Gulf Basin. A = Jiaowei Formation; B = Xiaying Formation; C = Weizhou Formation; D = Liushagang Formation, Member 1; E = Liushagang Formation, Member 2; F = Liushagang Formation, Member 3; G = Changliu Formation.

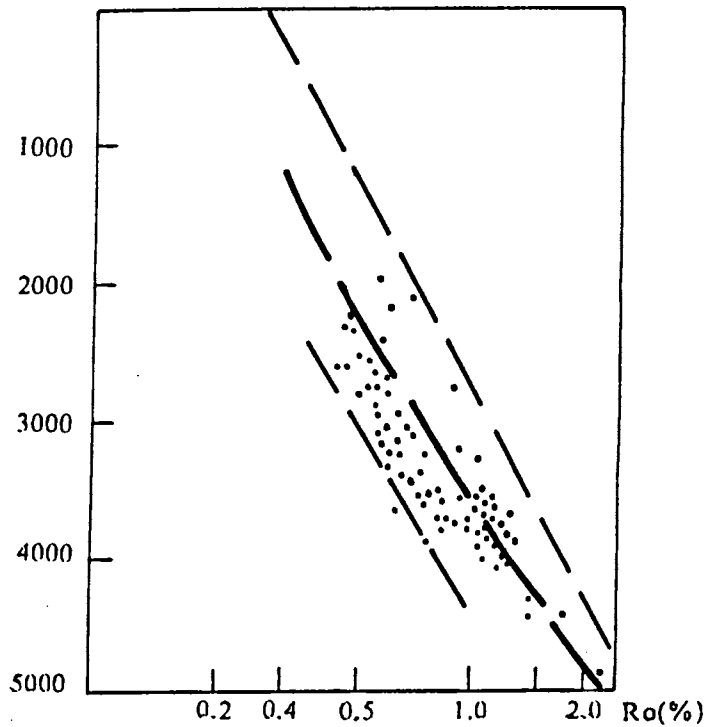


Figure 5. The vitrinite reflectance R_o distribution in the Yingge Sea and Qong Southeast Basin.

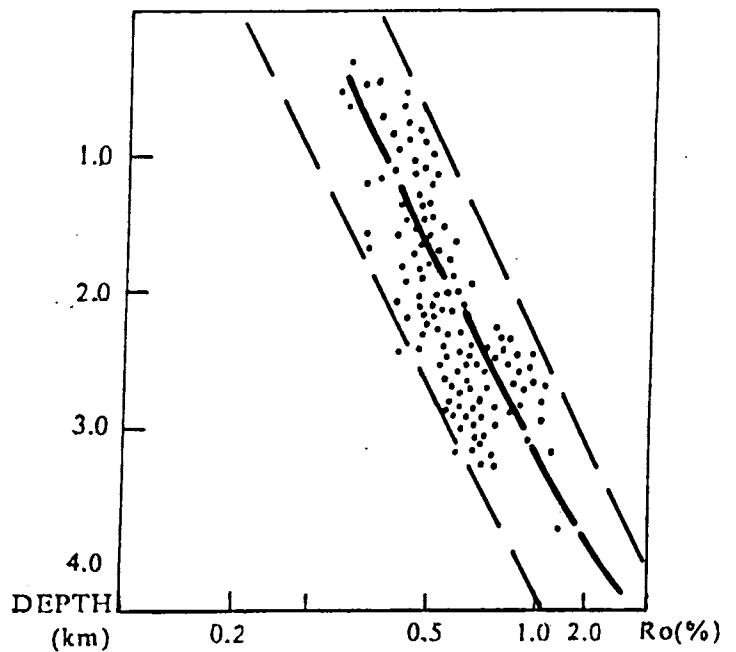


Figure 6. The vitrinite reflectance R_o distribution in Beibu Gulf Basin.

Vitrinite reflectance R_0 in the area

The vitrinite reflectance R_0 data in the areas are shown in Figures 5 and 6. As R_0 data can be disturbed by some factors such as erosion, water circulation, sediment interruption, sample selection and others, the least squares statistical analysis was used to obtain the relationship of R_0 data with depth. The relationship of R_0 with depth accepted in this paper is a regional function that may not be valid in some local areas. Therefore, the derived thermal evolution is also a regional event that applies on a basin-wide scale.

DISCUSSION

Based on the inversion method of geothermal history mentioned above with vitrinite reflectance R_0 data, hundreds initial heat flux profiles with time are produced randomly following the Monte Carlo method, and geothermal temperature profiles

are obtained using computer following the Simplex Method. Each geothermal temperature profile represents the best results in one run of inversion against one initial heat flux profile. The best geothermal temperature profile can be selected as the one which gives the smallest object function value. Figures 7 and 8 are inverse heat flux and geotemperature profiles in the Yingge Sea Basin and Beibu Gulf Basin. The profiles in Yingge Sea Basin are selected from 250 inversed runs, and the profiles in Beibu Gulf Basin are selected from 350 inversed runs.

R_0 data calculated from thermal temperature profiles have been compared to the measured values shown in Figure 5 and Figure 6. The two fit closely, especially in the data in Yingge Sea Basin (Fig. 9). The root mean square value is 0.0209 for the Yingge Sea Basin and 0.0908 for the Beibu Gulf Basin. The dispersion of the data points in the Beibu Gulf Basin could be due to the interruption of sedimentation since late Miocene and poor

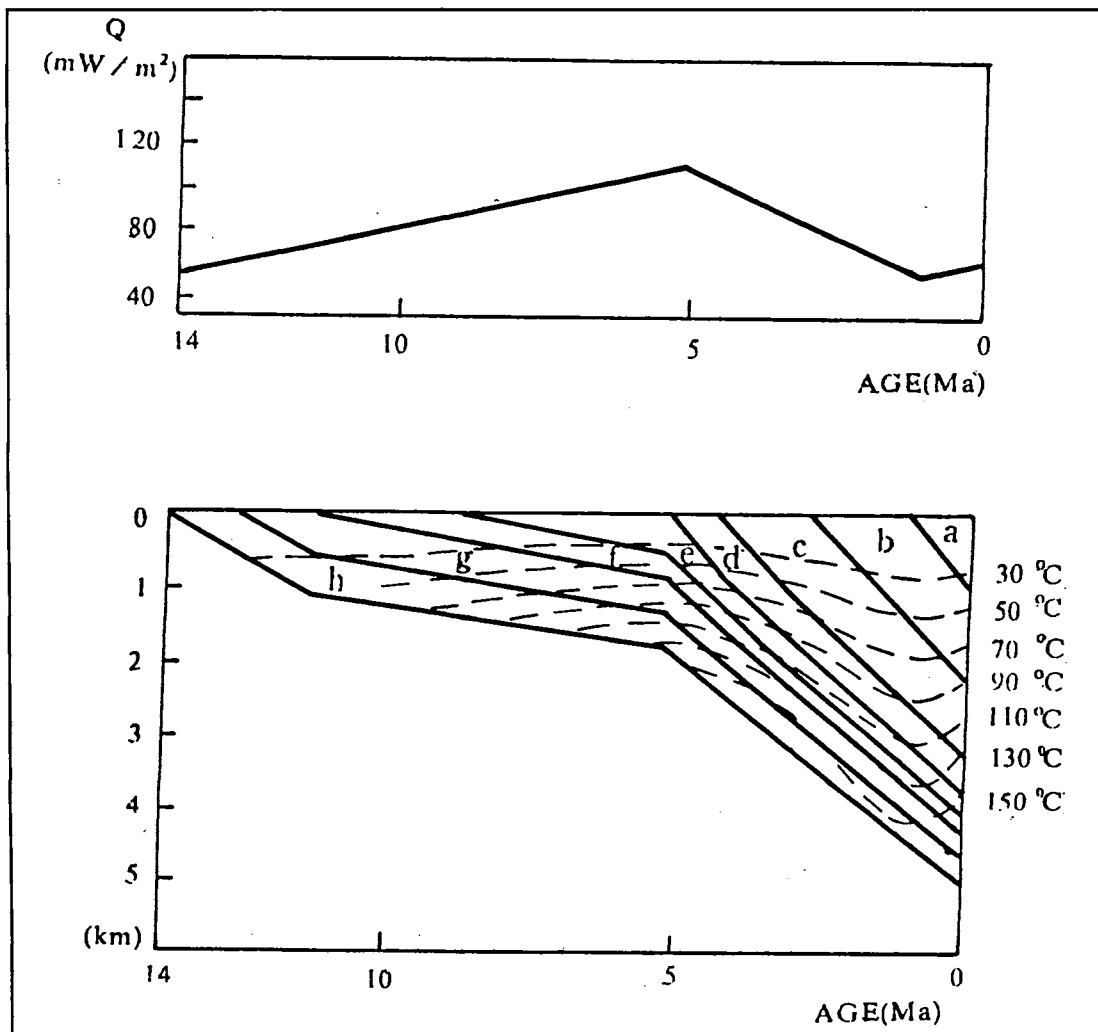


Figure 7. Thermal history evolution in Yingge Sea Basin. a-b: Quaternary; c-d: Pliocene (Yingge Sea Formation); e-f: upper Miocene (Huangliu Formation); g-h: middle Miocene (Meishan Formation)

subsidence history profiles studies of the basin. But, on a broad basinal scale, the modelling is considered sufficient to analyse the geothermal and tectonic evolution.

It is very clear that heat flux was increasing during the middle and upper Miocene, decreasing during the Pliocene and early Quaternary, and increased during late Quaternary in Yingge Sea Basin (Fig. 7). This geothermal evolution reflects tectonic evolution since early Miocene when the basin began to form. Although the Yingge Sea Basin began rifting in the early Miocene, the heat flux continue to increase. The event of anomalous heat flux tells us that the Yingge Sea Basin is not a simple extensional basin. After earlier Miocene when the basin broke up, northwest-directed strike faults in the basin may continue to be active and possibly the mantle continue to be uplifted. This may be the reason for the anomalous heat flux

during this time. At the beginning of Pliocene, the heat flux started to decrease, which may due to reduced tectonic activity since the middle Miocene. The large thickness of sediments characterise the geological record of the time. The subsidence may closely related to the geothermal decay. The increase of heat flux since 1-2 Ma may represent recent structural activity which is noted in the neighbouring northern part of Hainan Island.

The evolution of geothermal history in Gulf Basin is not same as that in the Yingge Sea Basin. The features of the heat flux profile are more like that for an extensional basin. The decrease of heat flux may have started during the Late Cretaceous or early Paleocene. During the upper Paleocene and lower Eocene, the heat flux continues to decay. The decrease of heat flux during the middle Oligocene may be due to reduced tectonic activities since the Late Eocene, the second tectonic stage.

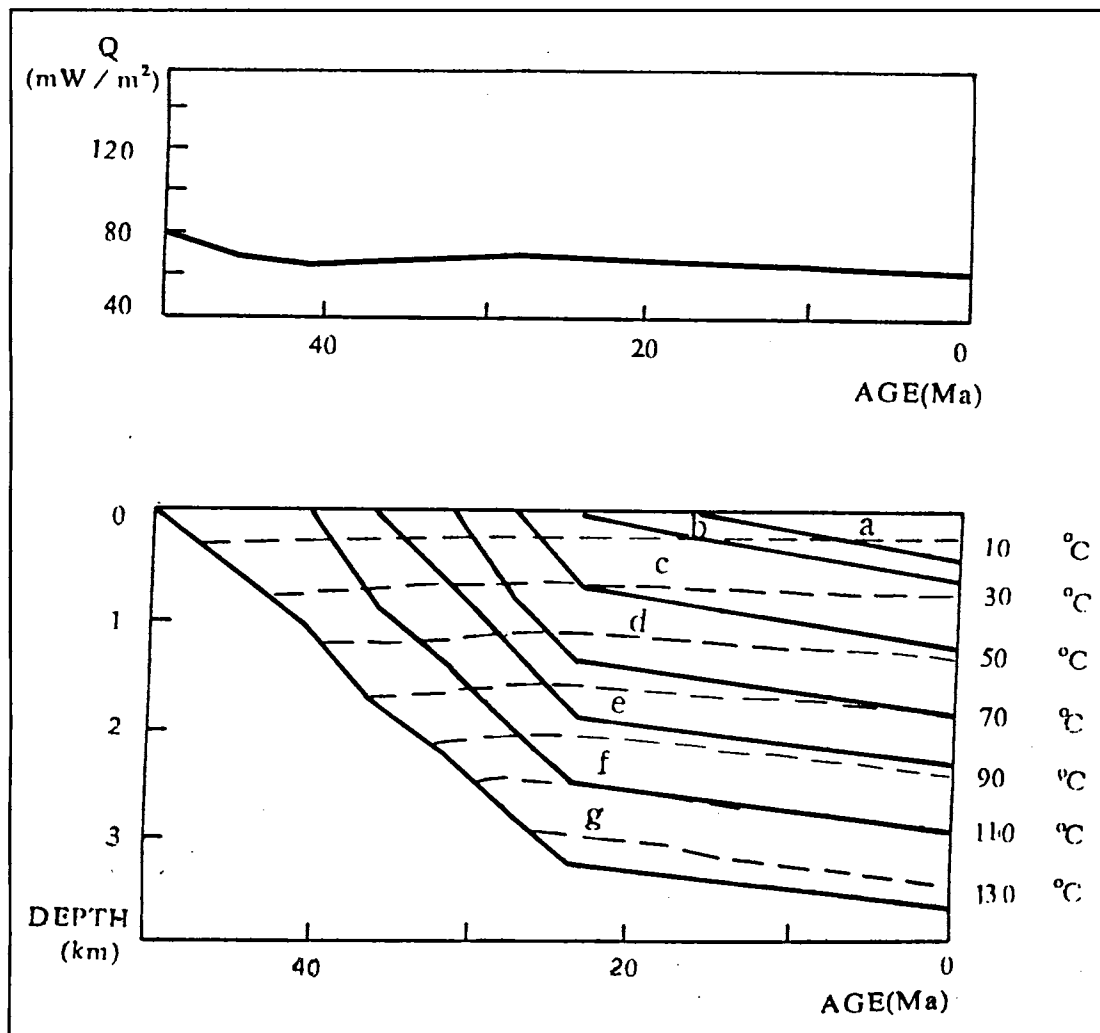


Figure 8. Thermal evolution of the Beibu Gulf Basin. a: middle Miocene (Jiaowei Formation); b: Lower Miocene (Xiaying Formation); c: middle upper Oligocene (Weizhou Formation); d: Lower Oligocene (Liushagang Formation Member 1); e: middle upper Eocene (Liushagang Formation Member 2); f: middle up Eocene (Liushagang Formation Member 3); g: Lower Eocene-Upper Paleocene (Changliu Formation).

The stages of tectonic activity in the northern part of south China Sea are reflected clearly in the geothermal evolution. At least two or three extensions and tectonic events have occurred since Late Mesozoic. From the features of the geothermal evolution, the author believes that Yingge Sea Basin is not a rift basin or an extensional basin, but a strike-slip and extensional basin. Many northwest-directed structures are recognised in the basin (Xue, *in prep*) are considered as Mesozoic structures. In its earlier stage, Yingge Sea Basin experienced extension like Qong Southeast Basin, Pearl River Mouth Basin and Beibu Gulf Basin. When Indian Plate and Eurasian Plate began to collide, the Yingge Sea Basin formed as a strike-slip and extensional basin along the northwest direction. The geothermal history inversion in the paper provides support for the presence of two kinds of basins in the northern part of the South China Sea.

From the geothermal temperature profile, the vitrinite reflectance R_0 profiles with time can be calculated based on equation given by Wood (1988),

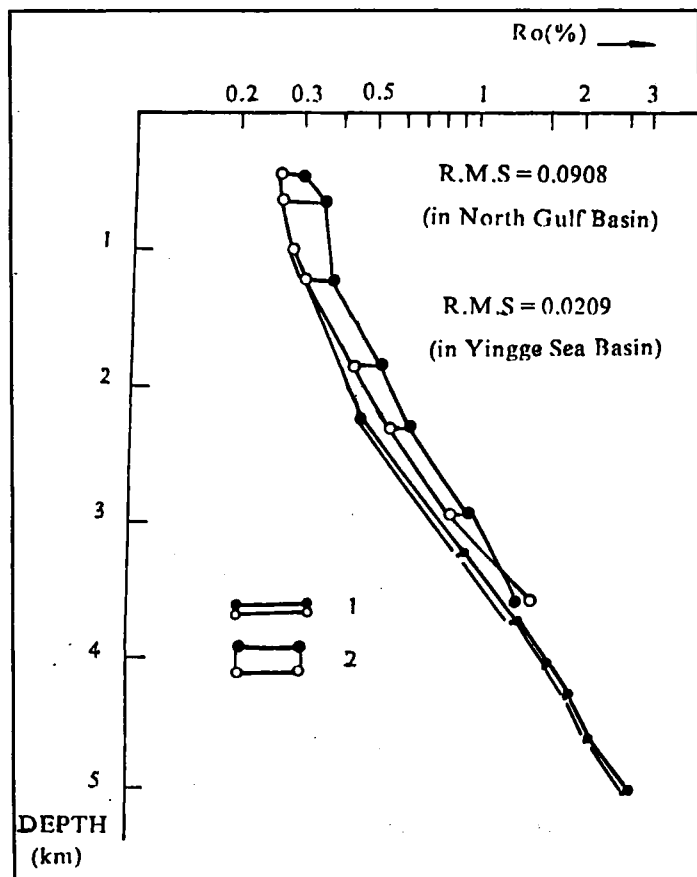


Figure 9. The comparison between measured and modelled R_0 in the northern part of the South China Sea.

- 1 = North Gulf Basin;
- 2 = Yingge Sea Basin;
- = Measured R_0 ;
- = Modeled R_0

and the oil window in which R_0 ranges from 0.65% to 1.3% in the Yingge Sea Basin and Beibu Gulf Basin are shown in Figure 10 and Figure 11. We note that as potential source rocks, Meishan formation in Yingge Sea Basin has overmatured and gas is the main resource target, but the Liushagang formation in Beibu Gulf Basin is mature and oil is the main resource target. The results of these calculations have been proved by exploration in some areas.

REFERENCES

- ALLEN, F.A. AND ALLEN, J.R., 1990. *Basin analysis, principles and applications*. Blackwell Scientific Publications.
- LERCHE, I., YARZARB, R.F. AND KENDALL, C.G. St. C., 1984. Determination of paleoheat flux from Vitrinite reflectance. *AAPG Bulletin*, 68, 1704-1717.
- LERCHE, I., 1988a. Inversion of multiple thermal indicators: Quantitative methods of determining paleoheat flux and geological parameters. I. The theoretical development for paleoheat flux. *Mathematical Geology*, 20, 1-36.
- LERCHE, I., 1988b. Inversion of multiple thermal indicators: Quantitative methods of determining paleoheat flux and geological parameters. II. The theoretical development for chemical, physical, and geological parameters. *Mathematical Geology*, 20, 73-96.
- LI Y. AND HUANG Z., 1990a. Thermal evolution of west part in the north shelf of South China Sea. *The Oil and Gas of Chinese Sea (Geology)*, 4(6), 31-39 (In Chinese).
- LI Y. AND HUANG Z., 1990b. Geothermal characteristics of the west part in the north shelf of South China Sea. *The Oil of South China Sea*, 7(a), 1-8 (In Chinese).
- LOPATIN, N.V., 1971. Temperature and geologic time as factors in colification. *Akademiya Nauk SSSR IZVESTIYA, Seriya Geologicheskaya*, 3, 95-106 (In Russian).
- LUTZ, T.M. AND OMAR, G., 1991. An inverse method of modelling thermal histories from apatite fission track data. *Earth and Planetary Science Letters*, 104, 181-185.
- McKENZIE, D., 1978. Some remarks in development of sedimentary basins. *Earth and Planetary Science Letters*, 40, 25-32.
- NUNA, J.A., SLEEP N.H. AND MOORE, W.E., 1984. Thermal subsidence and generation of hydrocarbons in Michigan basin. *AAPG Bulletin*, 68, 296-315.
- PANTANO, J. AND LERCHE, I., 1990. Inversion of Multiple thermal indicators: Quantitative methods of determining paleoheat flux and geological parameters. III. Stratigraphic age determination from inversion of vitrinite reflectance data and sterane isomerization data. *Mathematical Geology*, 22(3), 282-307.
- PRESS, W.H., FLANNERY, B.P., TEUKOLSKY, S.A. AND VETTERING, W.T., 1986. *Numerical Recipes the Art of Scientific Computing*. Cambridge University Press 1986.
- RU KE AND PIGOTT, J.D., 1985. South China Sea tectonic evolution and hydrocarbon potential: new geological and geophysical constraints (abs.). *AAPG Bulletin*, 69, 303.
- RU KE AND PIGOTT, J.D., 1986. Episodic rifting and subsidence in the South China Sea. *AAPG Bulletin*, 70, 1136-1151.

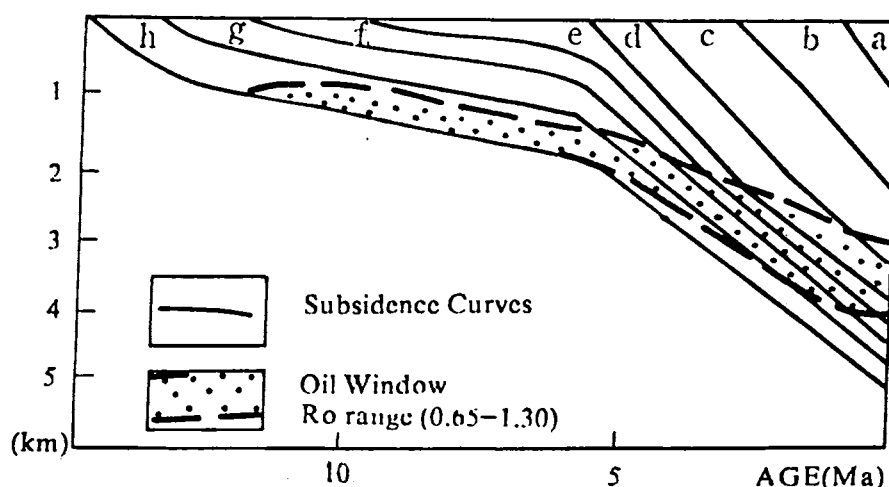


Figure 10. The oil window calculated for the Yingge Sea Basin.

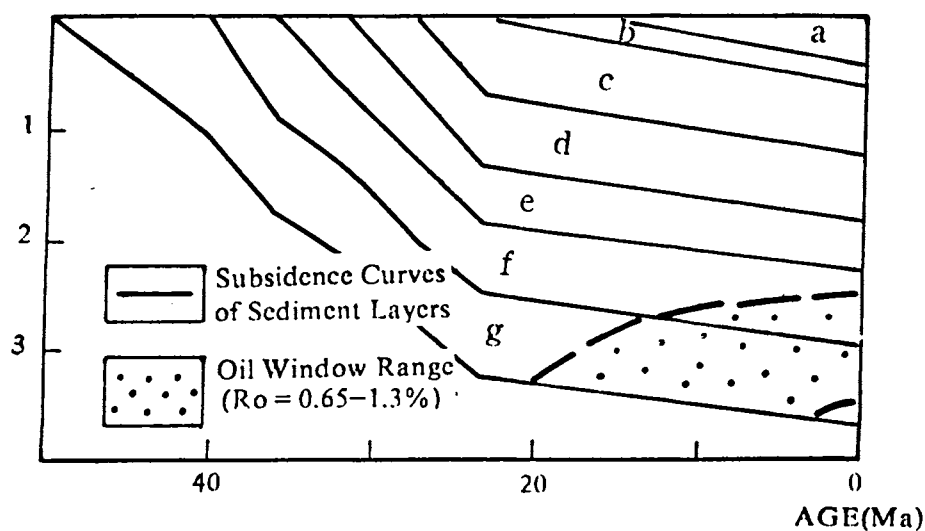


Figure 11. The oil window calculated for the Beibu Gulf Basin.

- RU KE AND FIGOTT, J.D., 1988. The development of superimposed basin on the northern margin of the South China Sea and its tectonic significance. *Oil and Gas Geology*, 9(1), 22-31 (In Chinese).
- ROYDEN, L. AND KEEN, C.E., 1980. Rifting process and thermal evolution of the continental margin of eastern Canada determined from subsidence curves. *Earth and Planetary Science Letters*, 51, 343-361.
- SASS, J.H., LACHENBRUCH, A.H. AND MUNROE, R.J., 1971. Thermal conductivity of rocks from measurements on fragments and its application to heat flow determination. *Denver, Rocky Mountain Association of Geologists Guide Book*, 41-54.
- XUE, A., (in preparation). The structural features of Yingge Sea Basin.
- WAPLES, D.W., 1980. Time and temperature in petroleum formation application of Lopatin method to petroleum exploration. *AAPG Bulletin*, 64, 916-926.
- WOOD, D.A., 1988. Relationships between thermal maturity indices calculated using Arrhenius Equation and Lopatin Method: Implications for Petroleum Exploration. *AAPG Bulletin*, 72, 115-134, 1988.